

Influence of fMRI smoothing procedures on replicability of fine scale motor localization

Alexander Geissler,^{a,b} Rupert Lanzenberger,^{a,b} Markus Barth,^a Amir Reza Tahamtan,^{a,b}
Denny Milakara,^{a,b} Andreas Gartus,^{a,b} and Roland Beisteiner^{a,b,*}

^aStudy Group Clinical fMRI at the Departments of Neurology and Radiology, Medical University of Vienna, Währinger Gürtel 18-20, A-1090 Vienna, Austria

^bLudwig Boltzmann Institute for Functional Brain Topography, Medical University of Vienna, A-1090 Vienna, Austria

Received 3 February 2004; revised 27 August 2004; accepted 30 August 2004
Available online 10 December 2004

Recent publications analyzing the influence of spatial smoothing on fMRI brain activation results demonstrated that smoothing may artificially combine activations from adjacent though functionally and anatomically distinct brain regions and that activation from large draining vessels may be smoothed into neighboring neuronal tissue. To investigate whether functional localizations may be artificially shifted by the smoothing procedure we performed replicability measurements. Localization centers of motor hand activations achieved during different conditions (isolated hand movements and simultaneous hand and chin movements) were compared with respect to smoothing effects. The voxel with the highest probability to represent a true positive activation was localized with a non-smoothed and a standard $4 \times 4 \times 6$ mm smoothed correlational data analysis technique. Results show an increase of motor center aberrations between measurements by about 100% due to data smoothing indicating a statistically significant decrease in localization replicability.

© 2004 Elsevier Inc. All rights reserved.

Keywords: fMRI; Functional resolution; Data smoothing; Motor localization; Replicability; Normal subjects; Patients

Introduction

In primary motor cortex and other essential cortical areas, the functional significance of neuronal tissue may change within millimeters. Neurosurgical literature described that a mean change in resection margins by about 1 cm may decide between no or permanent postoperative functional deficits and the transfer of a reversible to a permanent deficit is associated with a mean shift of

resection margins by only about 1 mm (Haglund et al., 1994). In addition, fine scale somatotopic investigations using fMRI demonstrated that representation centers for different finger movements may be only 2–3 mm apart (Beisteiner et al., 2001; Hlustik et al., 2001; Indovina and Sanes, 2001). As a consequence, a localization change of fMRI activations due to spatial smoothing might be problematic. Since recent studies analyzing the influence of spatial smoothing on fMRI brain activation results (Fransson et al., 2002; White et al., 2001) imply that such artificial localization changes may occur, we were interested whether smoothing procedures—as often used in clinical studies (Lawrie et al., 2002; Rocca et al., 2002; Staffen et al., 2002)—affect the localization of functional centers. Extraction of functional centers refers to previous publications on hand motor localization (Beisteiner et al., 2000) and Broca language area localization (Rutten et al., 1999) which indicate that within extended representation areas single voxels with the largest probability for a true positive may be defined which correlate best with intraoperative cortical stimulation. Knowledge about localization of such a functional center is important for clinical studies, since it represents the area of the highest risk for a postoperative functional deficit when damaged.

We examined the replicability of the hand motor center with a non-smoothed and a smoothed data analysis technique using standard smoothing values. To test the center stability under difficult circumstances—namely with varying overall activation patterns—two different movement conditions were used. Isolated hand movements were compared with simultaneous hand and chin movements. Chin movements are of clinical relevance for overt speech studies and are prone to produce head motion artifacts which might influence motor center replicability differently with regard to the amount of data smoothing.

In extension to previous studies (e.g., White et al., 2001), this study presents the first investigation of smoothing effects on fine scale localization using replicability measurements. To allow inferences about clinical relevance, two patients have been included and data are analyzed individually. Anatomical localization errors

* Corresponding author. Study Group Clinical fMRI at the Departments of Neurology and Radiology, Medical University of Vienna, Währinger Gürtel 18-20, A-1090 Vienna, Austria. Fax: +43 1 40400 3141.

E-mail address: roland.beisteiner@meduniwien.ac.at (R. Beisteiner).

Available online on ScienceDirect (www.sciencedirect.com).

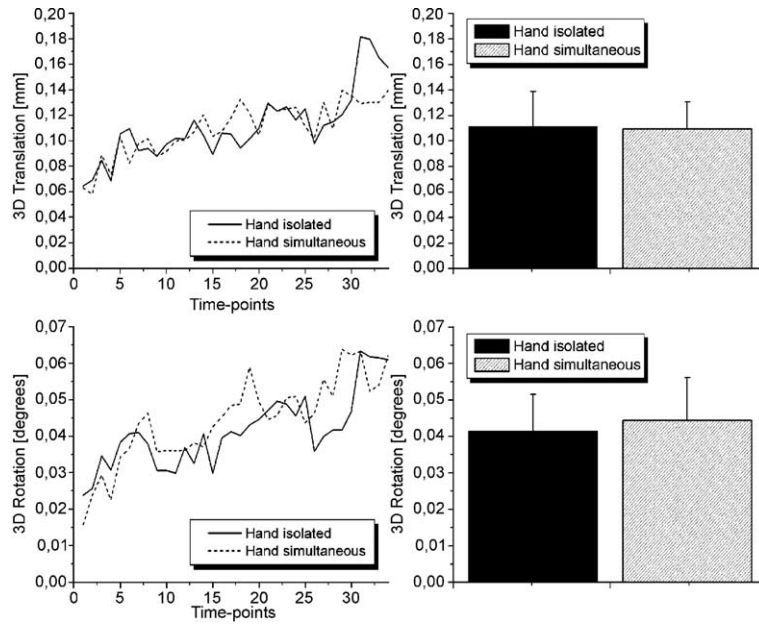


Fig. 1. Subject AU. Head motion quantification for each condition (hand isolated = continuous line/black bar, hand simultaneous = dotted line/grey bar). Top: translational head motion averaged over all three spatial dimensions and all runs, bottom: rotational head motion averaged over all three rotational axes and all runs. Left side shows time course of head position over the 35 image volumes (=time points) relative to initial position (first image volume). Right side shows average head displacement over all time points with the corresponding standard deviations. This subject showed the smallest overall head motion. No significant difference between conditions was found.

(White et al., 2001) are avoided by analyzing functional activations without normalization directly on original EPI images.

Materials and methods

Subjects/patients

11 healthy right handed subjects (mean age: 25.3 years; 7 male/4 female) and two right handed patients (mean age: 37.5

years; 1 male/1 female) participated in this study. Patient FI suffered a recurrence of a left frontoparietal astrocytoma II detected during routine MR diagnostics 3 months after first operation. Initially, the patient had presented with an epileptic seizure but was seizure free postoperatively. The postoperative local defect measured 2.8 cm in diameter. Patient HP suffered a 7 × 6.5 × 5.5 cm left parietooccipital glioblastoma. Initially, he presented with mnemonic deficits, lack of concentration and troubles with vision. He never experienced epileptic seizures. Both patients were in good general health, free of neurological deficits

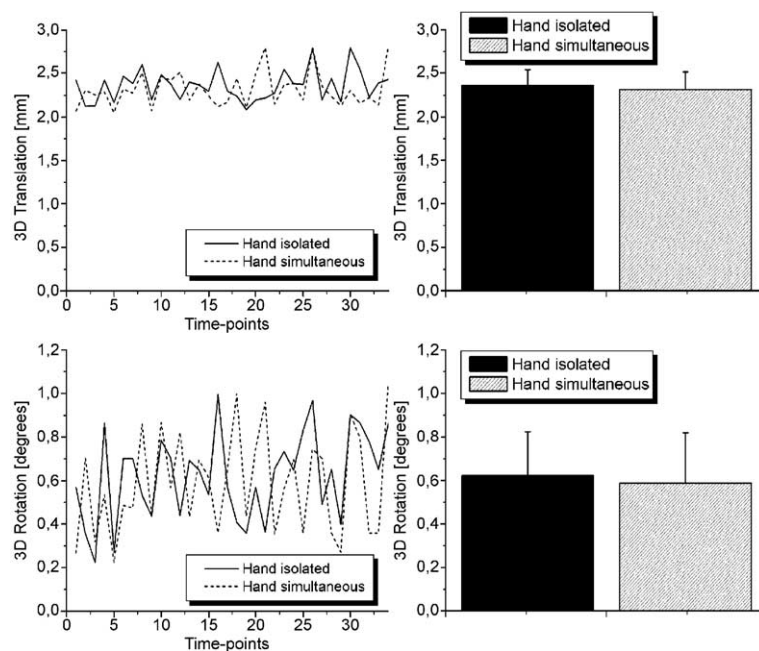


Fig. 2. Subject BJ. Same conventions as in Fig. 1. This subject showed the largest overall head motion. No significant difference between conditions was found.

at the time of fMRI investigations, and transferred for localization of the motor strip. The study was approved by the local ethics committee, and all subjects and patients gave written informed consent.

Task

Subjects performed two paradigms: (1) opening and closing of the right hand (condition hand isolated), (2) opening and closing of the right hand and chin simultaneously (condition hand simultaneous). For control 7 of the subjects also performed isolated chin movements. The movements were self-initiated and self-paced at a subjective convenient frequency using no explicit movement standardization. One run consisted of four rest and three movement phases with 20 s duration each. Depending on subject cooperation 6–7 runs were accomplished per condition. Start, stop, and type of movements were indicated to the subjects by acoustic commands via earphones.

MRI acquisition

To minimize head motion artefacts individually constructed plaster cast helmets were used for optimized and secure head fixation (Edward et al., 2000). fMRI measurements were done on a 3T BRUKER Medspec scanner (BRUKER Biospin, Ettlingen, Germany). We used a phase corrected single-shot, blipped GE-EPI sequence (TE/TR = 55.5/4000 ms, 128×128 matrix, 230×230

FOV, 25 axial slices, slice thickness 3 mm, voxel size $1.8 \times 1.8 \times 3$ mm, no interslice gap, sinc-pulse excitation).

MRI data analysis-post processing

Prior to further analysis, all volumes of every subject were realigned using AIR 3.08 (Woods et al., 1998) with a rigid 6 parameter (three transformation and three rotation parameters) model using a four step procedure: (1) The first volumes of all runs were realigned to the first volume of the first run. (2) The volumes of each run were realigned to the first volume of the same run. (3) For each run, the transformation obtained in step 1 was combined with the transformations from step 2, resulting in summary to a realignment of volumes of all runs to the first volume of the first run. (4) Finally, all volumes are repositioned to reflect the average position, size and shape of the volumes. Since we used anisotropic voxels of size $1.8 \times 1.8 \times 3$ mm AIR motion correction was done with a smoothing kernel of $4 \times 4 \times 0$ mm. AIR results were used to check head motion behavior of the subjects for each condition. Cumulating the aberration of the head position from the initial position along all spatial axes for each time point allowed to test for differences of mean head position between hand movement conditions using a *t* test after proving of normal data distributions by Kolmogorov–Smirnov tests. Figs. 1 and 2 depict the subjects with the lowest and largest overall head motion, respectively.

For both conditions, motor functional centers were defined within the primary motor cortex hand area as follows.

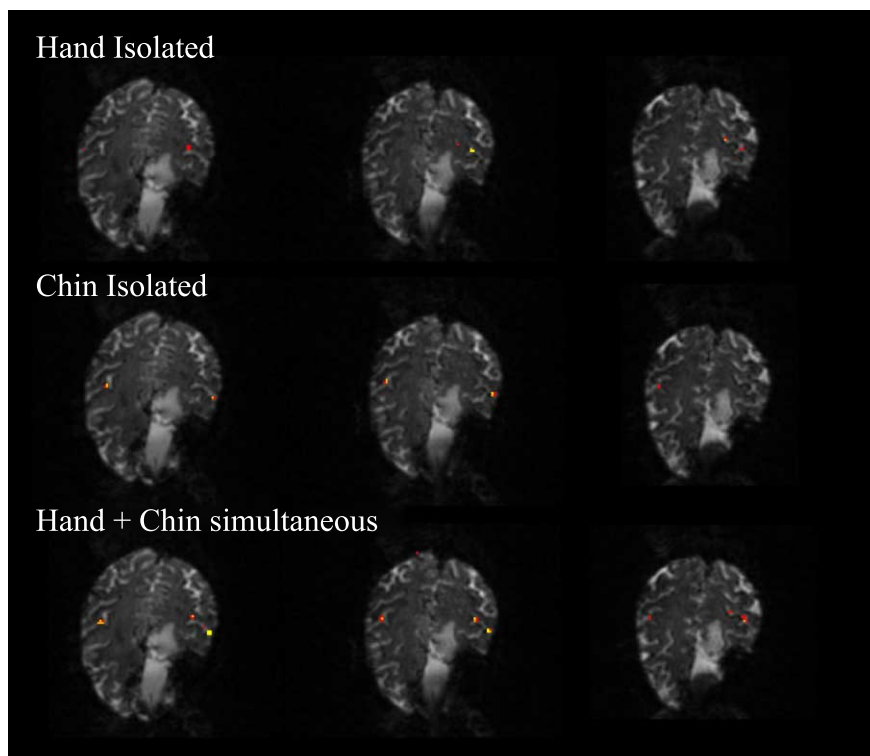


Fig. 3. Patient FI. Representation of the hand and chin areas on original EPI images (interpolated to 256×256) with non-smoothed risk maps. Colors indicate voxel reliability (yellow = most, red = least reliable, see text). According to the risk map procedure map specific correlation thresholds are $r > 0.65$ (hand isolated, chin isolated), $r > 0.55$ (hand + chin simultaneous). Note the clear separation of hand and chin activations visible in the middle column despite difficult fMRI conditions due to large pathology producing considerable susceptibility artefacts. For visualization all active risk map voxels are shown (no ROI).

SPM99 analysis

Since the least degree of smoothing that is compatible with the smoothness being large enough to ensure the validity of the statistical inferences is two times the voxel size, we performed SPM99 (<http://www.fil.ion.ucl.ac.uk/spm/>) analyses with a $4 \times$

4×6 mm FWHM Gaussian smoothing kernel. All scans of the same condition were analyzed together. The smoothed data were calculated with a fixed response box car function shifted by 8 s and not convolved with a hemodynamic response function. t value maps were generated depicting all voxels with positive t values (see Figs. 4 and 5) without using additional

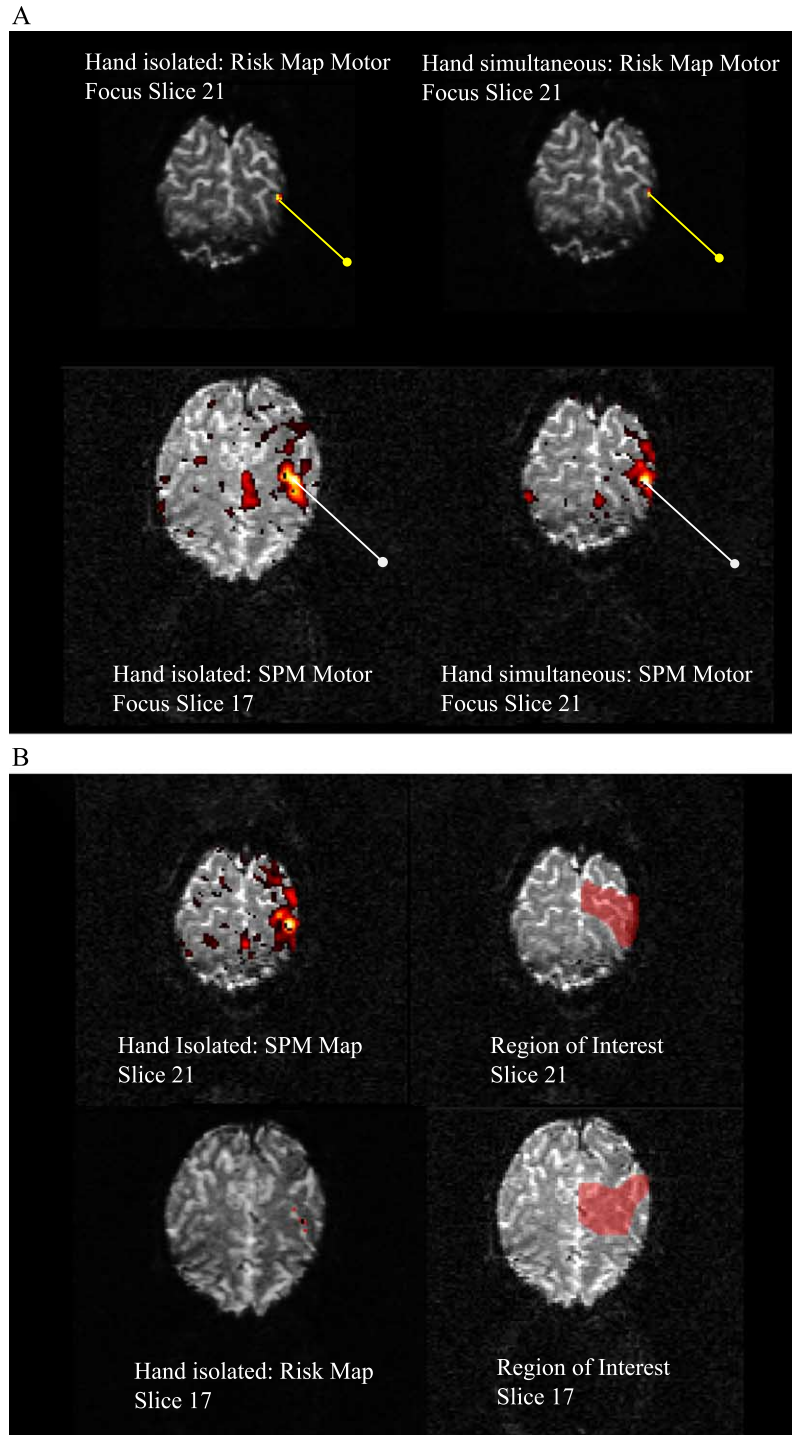


Fig. 4. (A) Subject BJ. Localization of the hand motor center with non-smoothed risk map (top) and 4 mm smoothed SPM techniques. The motor center is pinned. Functional activations are shown on original EPI images. Risk map specific correlation thresholds are $r > 0.6$ (hand isolated) and $r > 0.7$ (hand simultaneous). SPM maps show all voxels with positive t values (no p value thresholding). Motor center aberration with risk maps = 0 mm, with SPM 4 mm smoothing = 12 mm. (B) Subject BJ. Left: Corresponding SPM maps/risk maps missing in A. Right: Corresponding hand ROIs.

criteria in particular without P value thresholding. The primary motor cortex hand area was defined according to anatomic criteria (Yousry et al., 1997). Regions of interest (ROI) for the

hand area were drawn individually based on EPI and high resolution anatomical images and comprised the whole inverted omega structure as well as the pre- and postcentral gyrus—the

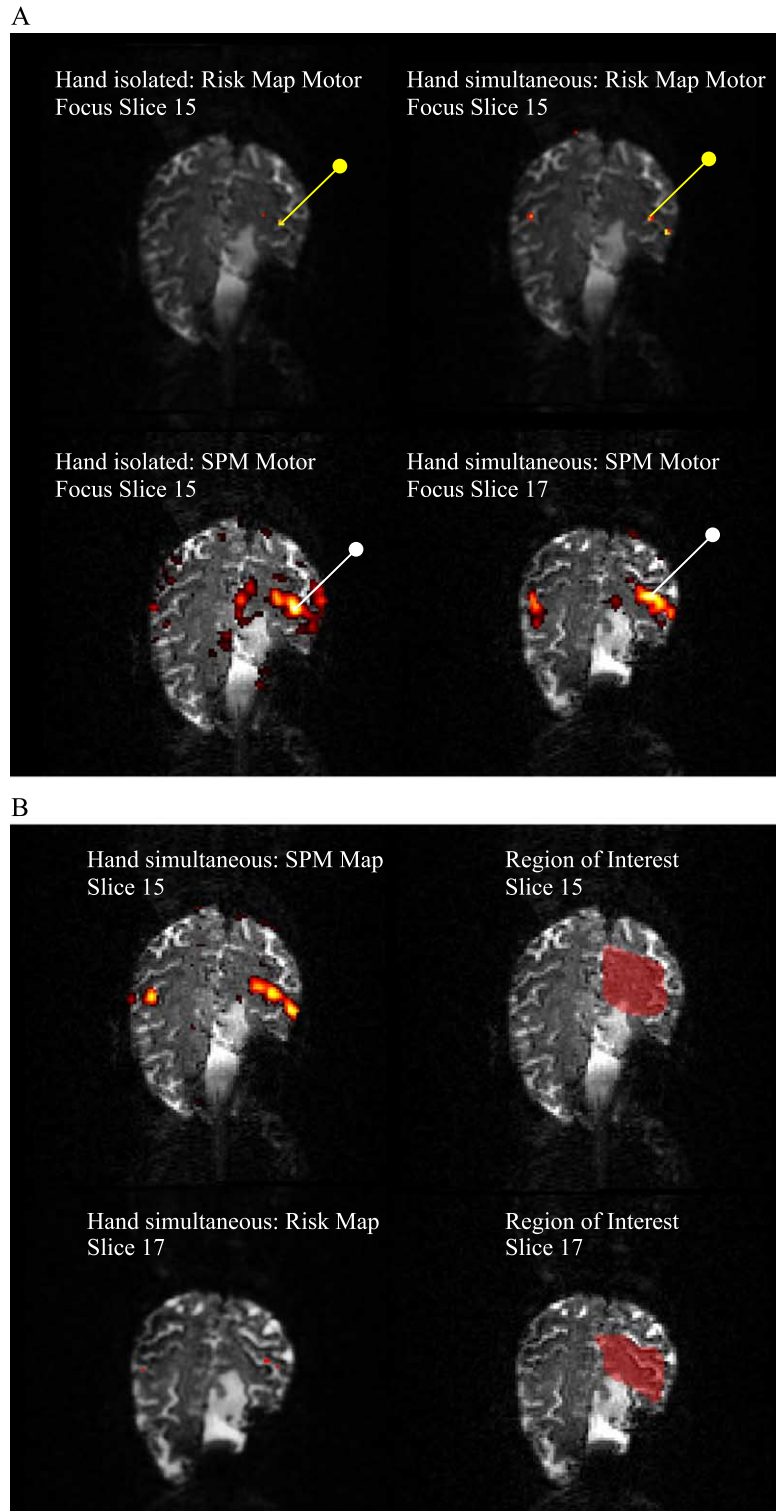


Fig. 5. (A) Patient FI. Same conventions as in Fig. 4A. Risk map-specific correlation thresholds are $r > 0.65$ (hand isolated) and $r > 0.55$ (hand simultaneous). Motor center aberration with risk maps = 1.8 mm, with SPM 4 mm smoothing = 10 mm. Note difficult fMRI conditions due to pathology related susceptibility artifacts. Nevertheless, smoothing effects on motor center aberration are comparable to normal subjects. (B) Patient FI. Left: Corresponding SPM maps/risk maps missing in A. Right: Corresponding hand ROIs.

Table 1
Individual localization differences of motor centers between isolated and simultaneous hand movements in mm

Subject	Difference risk map				Difference SPM 4 mm			
	Hand isolated vs. Hand simultaneous				Hand isolated vs. Hand simultaneous			
	ml	ap	si	3D dist	ml	ap	si	3D dist
BJ	0	0	0	0	0	0	-12	12
GS	-1.8	0	0	1.8	-1.8	1.8	0	2.55
HP	0	0	0	0	5.4	-5.4	-6	9.71
KI	1.8	-1.8	0	2.546	0	-1.8	0	1.8
LR	0	0	0	0	0	0	0	0
FI	0	-1.8	0	1.8	3.6	-7.2	-6	10
SC	0	0	0	0	-1.8	-1.8	0	2.55
AM	0	-1.8	-6	6.264	-1.8	-1.8	-6	6.52
LuR	-5.4	18	3	19.03	-3.6	3.6	-6	7.87
MG	-1.8	1.8	0	2.546	3.6	0	-3	4.69
SL	0	1.8	0	1.8	-1.8	5.4	0	5.69
TN	0	1.8	0	1.8	-1.8	1.8	3	3.93
TH	1.8	3.6	0	4.025	-3.6	-12.6	-9	15.9

The ml = medio-lateral, ap = anterior-posterior, si = superior-inferior axis and the 3D distances are given. The two patients are in bold type.

latter being known to comprise about 10–20% of the pyramidal tract axons. Identical ROIs were used for all analysis procedures. Corresponding to previous literature (e.g., Lotze et al., 2000), the voxel with the highest ROI *t* value (SPM *T* maps) was determined as the hand motor center. Since we did not investigate voxel clusters but peak values of the *t* maps, no statistical analysis was performed.

Non-smoothed data analysis

Previously, a high spatial resolution data analysis technique was introduced which allows separate evaluation of voxel reliability and mean correlation coefficient (Beisteiner, 2004; Beisteiner and Barth, in press; Beisteiner et al., 2000, 2001). Using the same reference function and the same ROIs as in SPM, a cross-correlation was calculated for every run. Voxel reliability was determined as the number of runs a voxel surpassed a certain correlation threshold. At various correlation thresholds reliability values were color coded and mapped as follows: yellow = 75–100% of runs active, orange = 50–75% of runs active, red = 25–50% of runs active (see Figs. 3,4,5). Since reliability values indicate voxels at largest risk for a specific functional deficit when damaged, these maps were previously called fMRI risk maps

Table 2
Mann–Whitney–Wilcoxon *U* test results testing for increases in 3D differences between non-smoothed and smoothed analysis techniques

	Non-smoothed RiskMap versus SPM99 4 mm smoothing Total group data (13 subjects)
Double sided significance	0.022
	Non-smoothed RiskMap versus SPM99 4 mm smoothing Healthy subgroup data (11 subjects)
Double sided significance	0.116

(Beisteiner et al., 2000). Based on the risk maps, the hand motor center was found by searching the largest correlation threshold that yielded an ROI voxel with a reliability of 75–100%. Hand and chin activations were clearly separable on the risk maps for all subjects (see Fig. 3) when analyzing combined anatomical and functional information. This assured correct assignment of hand activations and chin activations (compare Figs. 4 and 5).

Statistical analysis

For each subject and every data analysis technique localization differences of the hand motor center between conditions were calculated in 3D. The 3D distance was defined as the length of the distance vector spanned between the isolated and the simultaneous hand movement center. The Euclidean distance was calculated as $\sqrt{(x_1 - x_2)^2 + (y_1 - y_2)^2 + (z_1 - z_2)^2}$, where x_1, y_1, z_1 and x_2, y_2, z_2 are the Cartesian coordinates of the hand motor center in the simultaneous and isolated conditions, respectively. The calculated differences establish the replicability between conditions and are given in Table 1 in detail. To test for an analysis specific difference of 3D distances a Wilcoxon test was performed comparing the smoothed with the non-smoothed data analysis technique for the whole group and for the healthy subgroup of normal subjects only (see Table 2). Mean 3D distances are given in Table 3. Tables 4 and 5 show the corresponding Talairach coordinates for every motor center achieved after normalization of the data with SPM99 using the EPI template. Wilcoxon tests were also performed with these data.

Table 3
Mean 3D distances per analysis method in mm (compare Fig. 6)

3D Distance total group (13 subjects)	Mean	Standard deviation
RiskMap	3.39	5.26
SPM 4 mm	6.4	4.56
3D Distance healthy subgroup (11 subjects)	Mean	Standard deviation
RiskMap	3.65	1.53
SPM 4 mm	5.77	1.42

Table 4

Voxel coordinates and associated Talairach coordinates as resulting from the non-smoothed risk map analysis

Subject	Voxel coordinates						Talairach coordinates					
	Hand isolated			Hand simultaneous			Hand isolated			Hand simultaneous		
	ml	ap	si	ml	ap	si	ml	ap	si	ml	ap	si
BJ	83	88	21	83	88	21	32	44	58	32	44	57
GS	88	78	23	89	78	23	-36	-11	62	-38	-11	62
HP	77	54	29	77	54	29	-25	-55	65	-25	-55	64
KI	91	54	19	90	55	19	-39	-19	50	-37	-18	51
LR	79	70	19	79	70	19	-30	-1	49	-30	-1	49
FI	88	66	15	88	67	15	-36	-10	45	-36	-9	45
SC	81	48	23	81	48	23	-29	-12	42	-28	-12	42
AM	90	72	20	88	75	22	-27	-9	55	-22	-5	64
LuR	94	75	21	97	66	20	-40	-14	59	-46	-36	51
MG	81	69	24	82	68	24	-34	-19	68	-36	-21	67
SL	90	73	20	90	72	20	-51	33	31	-51	31	32
TN	92	64	19	92	63	19	-55	-33	44	-55	-36	43
TH	83	73	23	82	71	23	-35	-20	63	-34	-25	62

The voxel coordinates are pure matrix coordinates without consideration of the voxel dimension. Here MRIcro (Rorden, C.) convention was used (point of origin: bottom left corner).

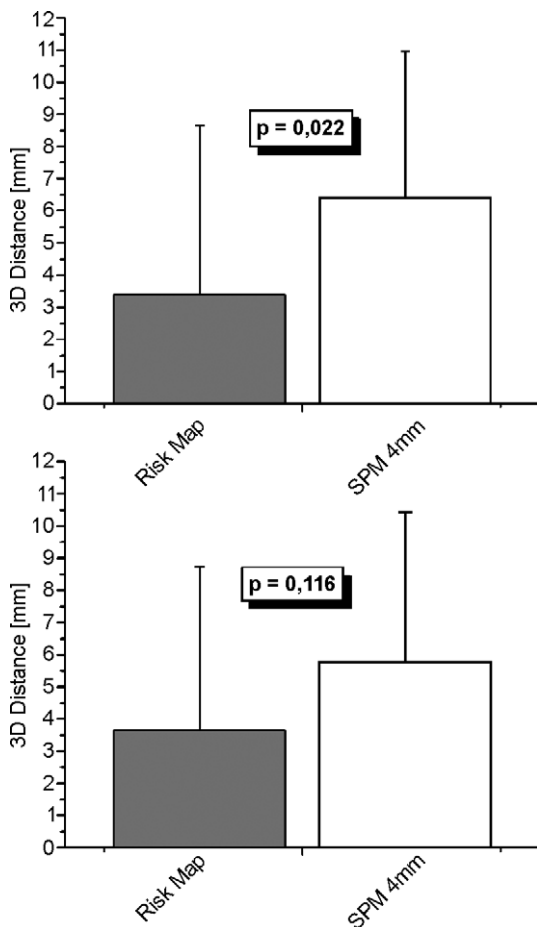


Fig. 6. Bar graph illustration of the mean and standard deviations of the 3D distances of hand motor centers for isolated and simultaneous movements. The influence of functional data smoothing with SPM 4mm smoothing Kernel is shown. Top: total group data (13 subjects), bottom: healthy subgroup (11 subjects).

Results

Analysis of head motion behavior showed generally low motion effects and no difference between conditions. The mean time course of head motion over all runs is shown in Fig. 1 for the subject with the smallest and in Fig. 2 for the subject with the largest overall head motion. Kolmogorov–Smirnov tests indicated normally distributed data and *t* tests revealed no significant differences between condition related head motion for neither subject and neither motion form (translation, rotation).

Localizations for hand and chin activity were found in primary motor areas corresponding to the motor homunculus as previously described. A separation of hand and chin clusters was possible with every subject (see Fig. 3). Smoothing-dependent differences of the movement representation centers for isolated and simultaneous movements are depicted in Table 1 and Fig. 6. With smoothing, the mean 3D distance between motor centers increased by about 100% (Table 3) and in 10/13 subjects motor center replicability deteriorated (Table 1). The increase of 3D distances with smoothing was statistically significant for the total group data (Table 2). Since the patients (HP, FI) exhibited very large smoothing related distance increases, a subanalysis of normal subjects only showed the same trend but did not reach significance (Table 2, Fig. 6). When calculating statistics after data normalization using the Talairach coordinates (Tables 4 and 5), the same behavior with nearly identical statistical values was found.

Discussion

Recent publications analyzing the influence of spatial smoothing on fMRI brain activation results (Fransson et al., 2002; White et al., 2001) demonstrated that smoothing may artificially combine activations from adjacent though functionally and anatomically distinct brain regions and activation from large draining vessels may be smoothed into neighboring neuronal tissue. This implies that functional localizations may be artificially shifted by the smoothing procedure. To investigate this issue in more detail, we compared cortical representations

Table 5
Results for the 4-mm smoothed SPM analysis

Subject	Voxel coordinates						Talairach coordinates					
	Hand isolated			Hand simultaneous			Hand isolated			Hand simultaneous		
	ml	ap	si	ml	ap	si	ml	ap	si	ml	ap	si
BJ	83	88	17	83	88	21	-34	-36	43	-32	-44	57
GS	93	75	21	94	74	21	-46	-12	53	-48	-14	53
HP	80	50	27	77	53	29	-30	-56	54	-25	-56	63
KI	90	59	20	90	60	20	-35	-11	56	-35	-9	57
LR	79	70	19	79	70	19	-30	-1	49	-30	-1	49
FI	88	66	15	86	70	17	-36	-10	45	-31	-5	53
SC	80	48	23	81	49	23	-26	-12	42	-28	-10	41
AM	90	72	20	91	73	22	-27	-9	55	-28	-9	64
LuR	92	77	19	94	75	21	-37	-7	51	-40	-14	59
MG	84	69	23	82	69	24	-38	-19	63	-36	-19	68
SL	89	75	20	90	72	20	-49	37	29	-51	31	32
TN	92	64	20	93	63	19	-55	-34	48	-56	-36	43
TH	81	65	19	83	72	22	-33	-32	41	-35	-21	59

Same conventions as in Table 4.

of movements performed by the same effector under varying movement conditions and analyzed with a high spatial resolution and a standard smoothing approach. Without smoothing, localization errors due to noise effects should be minimized since scattered noise voxels do not affect the true response when only the most active voxel is evaluated. Our risk map technique applied here specifically evaluates voxel reliability and extracts the voxel with the highest probability for a true positive activation within the given experimental context. This motor center definition has already been validated by comparison with intraoperative cortical stimulation (Beisteiner et al., 2000) and is routinely used for clinical localization purposes. We found a significant decrease in localization replicability due to standard data smoothing. Motor center aberrations increased by about 100% with data smoothing. Interestingly, the two patients were among the subjects with the largest deterioration of replicability calling for special caution with clinical data analysis. Using the risk map technique, one patient showed perfect replicability of the hand motor center the other differed only at 1 voxel coordinate. With 4 mm smoothing motor centers differed by 9.71 mm (3D distance, patient HP) and 10 mm (3D distance, patient FI) between conditions. The most likely reason for patients unfavorable behavior is a larger noise level due to reduced capabilities for cooperation (Beisteiner, 2004; Beisteiner and Barth, in press). Over the whole group, the maximum effect was observed with subject BJ where localization differences increased by 12 mm.

In general, our data indicate that more reliable fMRI localizations will be achieved with a non-smoothed data analysis technique. They also indicate that uncritical use of standard smoothing procedures may be problematic in a clinical environment. Of course, the impact of smoothing related localization shifts depends on the investigational goal. With cognitive tasks (e.g., language and memory localization) fine scale localization is often not as important as grossly localizing active areas. A typical situation here is the determination of hemispheric dominance where the consequences of smoothed data analysis pose mostly no problems. The same is true for group studies investigating mean group activations. A different situation exists when definition of an individual activation

maximum is required. Examples are fine scale somatotopic investigations or determination of essential neuronal tissue for a specific brain function such as movement. Preoperatively, essential tissue localizations need to be known for planning the best surgical approach and defining optimum resection margins. Although with current fMRI techniques, it is still not clear how the border between essential and non-essential activations can be drawn safely, the ability to define the location which is most probably truly active helps. Our data show that non-smoothed data analysis is advantageous to achieve this.

Acknowledgments

We want to acknowledge important general support by Prof. Lueder Deecke, Department of Clinical Neurology, Medical University of Vienna, Head Ludwig Boltzmann Institute for Functional Brain Topography and by Prof. Siegfried Trattig, Department of Radiology, Medical University of Vienna. This study was supported by the Austrian Science Foundation (P15102).

References

- Beisteiner, R., 2004. Indikationen, Probleme und Ergebnisse der funktionellen MRT im Kindesalter. *Pädiatrische Praxis* 64 (2), 285–298.
- Beisteiner, R., Barth, M., 2004. Probleme und Lösungsmöglichkeiten bei Patientenuntersuchungen mit funktioneller Magnetresonanztomographie (fMRT). In: Walter, H. (Ed.), *Funktionelle Bildgebung in Psychiatrie und Psychotherapie-Methodische Grundlagen und Klinische Anwendungen*. Stuttgart, Schattauer Verlag. In press.
- Beisteiner, R., Lanzenberger, R., Novak, K., Edward, V., Windischberger, C., Erdler, M., Cunnington, R., Gartus, A., Streibl, B., Moser, E., Czech, T., Deecke, L., 2000. Improvement of presurgical patient evaluation by generation of functional magnetic resonance risk maps. *Neurosci. Lett.* 290, 13–16.
- Beisteiner, R., Windischberger, C., Lanzenberger, R., Edward, V., Cunnington, R., Erdler, M., Gartus, A., Streibl, B., Moser, E., Deecke, L., 2001. Finger somatotopy in human motor cortex. *NeuroImage* 13, 1016–1026.

- Edward, V., Windischberger, C., Cunnington, R., Erdler, M., Lanzenberger, R., Mayer, D., Endl, W., Beisteiner, R., 2000. Quantification of fMRI artifact reduction by a novel plaster cast head holder. *Hum. Brain Mapp.* 11, 207–213.
- Fransson, P., Merboldt, K.D., Petersson, K.M., Ingvar, M., Frahm, J., 2002. On the effects of spatial filtering—A comparative fMRI study of episodic memory encoding at high and low resolution. *NeuroImage* 16, 977–984.
- Haglund, M.M., Berger, M.S., Shamseldin, M., Lettich, E., Ojemann, G.A., 1994. Cortical localization of temporal lobe language sites in patients with gliomas. *Neurosurgery* 34, 567–576.
- Hlustik, P., Solodkin, A., Gullapalli, R.P., Noll, D.C., Small, S.L., 2001. Somatotopy in human primary motor and somatosensory hand representations revisited. *Cereb. Cortex* 11, 312–321.
- Indovina, I., Sanes, J.N., 2001. On somatotopic representation centers for finger movements in human primary motor cortex and supplementary motor area. *NeuroImage* 13, 1027–1034.
- Lawrie, S.M., Buechel, C., Whalley, H.C., Frith, C.D., Friston, K.J., Johnstone, E.C., 2002. Reduced frontotemporal connectivity in schizophrenia associated with auditory hallucinations. *Biol. Psychiatry* 51, 1008–1011.
- Lotze, M., Erb, M., Flor, H., Huelsmann, E., Godde, B., Grodd, W., 2000. fMRI evaluation of somatotopic representation in human primary motor cortex. *NeuroImage* 11, 473–481.
- Rocca, M.A., Matthews, P.M., Caputo, D., Ghezzi, A., Falini, A., Scotti, G., Comi, G., Filippi, M., 2002. Evidence for widespread movement-associated functional MRI changes with PPMS. *Neurology* 58, 866–872.
- Rorden, C. MRICro available at: http://www.cla.sc.edu/psyc/faculty/rorden/MRICro_users_support_list <http://www.jiscmail.ac.uk/archives/mricro.html>. Calculations in this paper: MRICro 1.37, built 1.
- Rutten, G.J., van Rijen, P.C., van Veelen, C.W., Ramsey, N.F., 1999. Language area localization with three-dimensional functional magnetic resonance imaging matches intrasulcal electrostimulation in Broca's area. *Ann. Neurol.* 46, 405–408.
- Staffen, W., Mair, A., Zauner, H., Unterrainer, J., Niederhofer, H., Kutzelnigg, A., Ritter, S., Golaszewski, S., Iglseder, B., Ladurner, G., 2002. Cognitive function and fMRI in patients with multiple sclerosis: evidence for compensatory cortical activations during attention task. *Brain* 125, 1275–1282.
- White, T., O'Leary, D., Magnotta, V., Arndt, S., Flaum, M., Andreasen, N.C., 2001. Anatomic and functional variability: the effects of filter size in group fMRI data analysis. *NeuroImage* 13, 577–588.
- Woods, R.P., Grafton, S.T., Holmes, C.J., Cherry, S.R., Mazziotta, J.C., 1998. Automated image registration: I. General methods and intrasubject, intramodality validation. *Comput. Assist. Tomogr.* 22, 141–154.
- Yousry, T.A., Schmid, U.D., Alkadhi, H., Schmidt, D., Peraud, A., Buettner, A., Winkler, P., 1997. Localization of the motor hand area to a knob on the precentral gyrus. A new landmark. *Brain* 120, 141–157.